

Propofol modulates the proliferation, invasion and migration of bladder cancer cells through the miR-145-5p/TOP2A axis

YI DU*, XUDONG ZHANG*, HONGWEI ZHANG, YIDING CHEN, SHUYING ZHU, JINJUN SHU and HUI PAN

Department of Anesthesiology, Sichuan Cancer Hospital and Institute, Sichuan Cancer Center, School of Medicine, University of Electronic Science and Technology of China, Chengdu, Sichuan 610041, P.R. China

Received June 9, 2020; Accepted January 28, 2021

DOI: 10.3892/mmr.2021.12078

Abstract. Propofol-based anesthesia has been reported to reduce the recurrence and metastasis of a number of cancer types following surgical resection. However, the effects of propofol in bladder cancer (BC) are yet to be fully elucidated. The aim of the present study was to investigate the functions of propofol in BC and their underlying mechanisms. In the study, the expression of microRNA (miR)-145-5p in BC tissues and cell lines was evaluated using reverse transcription-quantitative PCR, and the effects of propofol on BC cells were determined using cell viability, wound healing and Transwell cell invasion assays, bioinformatics analysis, western blotting, immunohistochemistry and *in vivo* tumor xenograft models. It was found that propofol significantly suppressed the proliferation, migration and invasion of BC cells *in vitro*. In addition, propofol induced miR-145-5p expression in a time-dependent manner, and miR-145-5p knockdown attenuated the inhibitory effects of propofol on the proliferation, migration and invasion of BC cells. Topoisomerase II α (TOP2A) was a direct target of miR-145-5p, and silencing TOP2A reversed the effects of miR-145-5p knockdown in propofol-treated cells. Furthermore, propofol suppressed tumor xenograft growth, which was partially attenuated by miR-145-5p knockdown. The present study provided novel insight into the advantages of surgical intervention with propofol anesthesia in patients with BC.

Introduction

Bladder cancer (BC) is one of the most common malignancies of the urological system in males worldwide (1). It is a leading cause of morbidity and mortality, with nearly 400,000 new cases and 150,000 deaths worldwide (1). Risk factors for BC include chronic inflammation, genetic susceptibility, smoking, occupational exposure and environmental pollutants (2,3). It is estimated that 5-10% of patients with BC are diagnosed at the metastatic stage and 50% will develop distant metastasis after cystectomy (4). Radical cystectomy in combination with chemotherapy drugs, such as dacarbazine, platinum compounds and methotrexate, or immunotherapy drugs, such as atezolizumab (anti-programmed cell death protein 1 monoclonal antibody) and samalizumab (anti-CD200), are currently available methods for the treatment of BC; however, the prognosis of patients with BC remains poor due to high rates of recurrence and metastasis (5). Preclinical and clinical studies indicate that perioperative conditions, including the anesthetic agent used, can affect cancer recurrence, metastasis and overall survival of patients with cancer (6). Anesthetic agents have been shown to serve important roles in cell proliferation, apoptosis and angiogenesis (6,7).

Propofol is a frequently used intravenous anesthetic agent. A previous study reported that propofol-based anesthesia reduces the risk of recurrence and metastasis of a variety of cancers after surgery resection (7). A retrospective study showed that propofol-based anesthesia significantly decreased mortality rates due to its tumor-suppressive effects (8). Propofol is reported to suppress cell proliferation, migration and invasion, and induce apoptosis by regulating microRNA (miRNA/miR) molecules, such as miR-143 and miR-199a, as well as target proteins, such as SRY-box transcription factor 4 (9,10). In BC, the effects of propofol are controversial. For example, Zhang *et al* (11) reported the propofol-induced proliferation and invasion of BC cells via activation of the nuclear-related factor 2 signaling pathway. Therefore, the present study was conducted to explore the effects of propofol on BC cells, as well as to determine the underlying molecular mechanisms.

miRNA molecules are small non-coding RNA transcripts (19-25 nucleotides in length) (12). Aberrant miRNA expression has been observed in various types of cancer,

Correspondence to: Dr Hongwei Zhang, Department of Anesthesiology, Sichuan Cancer Hospital and Institute, Sichuan Cancer Center, School of Medicine, University of Electronic Science and Technology of China, 55 Section 4, Renmin South Road, Wuhou, Chengdu, Sichuan 610041, P.R. China
E-mail: zhanghongwei@sohu.com

*Contributed equally

Key words: propofol, invasion, migration, bladder cancer, microRNA-145-5p, topoisomerase II α

including BC (12). Among these miRNA molecules, miR-145-5p has been reported to have reduced expression and to be associated with the progression and development of BC tumors (13,14). Dyrskjöt *et al* (13) examine the miRNA expression profile of 106 BC samples using microarray and found miR-145 to be the most downregulated miRNA in BC. Dip *et al* (14) studied the expression profile of miR-145 in BC, and found it to be a candidate diagnostic marker. Pignot *et al* (15) evaluated the miRNA expression of 166 BC samples and found that miR-145 was among the 15 most dysregulated miRNA molecules. In addition, miR-145 acted as a tumor suppressor in BC cells and was involved in regulating hypoxia-dependent apoptosis and the Warburg effect (16-18).

Topoisomerase II α (TOP2A) is an enzyme that regulates the DNA topological state, breaks double-stranded DNA and induces gene transcription during mitosis (19). TOP2A is suggested to be involved in the development of several cancer types, such as pancreatic, breast and colon cancer (20-22). In pancreatic cancer, TOP2A induced the malignant transformation of cells by activating the β -catenin signaling pathway (21). The aim of the present study was to elucidate the underlying molecular mechanism of propofol in BC. The effects of propofol on BC cells were determined using cell viability, wound healing and Transwell cell invasion assays, bioinformatics analysis, western blotting, immunohistochemistry and *in vivo* tumor xenograft models.

Materials and methods

Clinical samples and cell culture. A total of 30 pairs of BC tissues and matched adjacent normal tissues (0.5 cm between BC tissues and normal tissues) were collected from patients with BC (40 to 75 years old, 17 male patients and 13 female patients who had not undergone chemotherapy before surgery) who received cystectomy between July 2018 and May 2019 at Sichuan Cancer Hospital & Institute (Chengdu, China). All samples were obtained after receiving informed consent from patients, and the study protocol was approved by the Ethics Committee of the University of Electronic Science and Technology of China [approval no. SYSK (Jing) 2018-0034]. The human BC cell lines J82 and T24, as well as the SV40 immortalized human uroepithelial cell line SV-HUC-1, were purchased from American Type Culture Collection, and cultured in RPMI-1640 medium (Gibco; Thermo Fisher Scientific, Inc.) supplemented with 10% FBC (HyClone; Cytiva) at 37°C in a humidified incubator containing 5% CO₂. These cell lines were verified via short tandem repeat profiling. Propofol was purchased from Shanghai Zhenrui Biotechnology Co., Ltd., and diluted in DMSO (Sigma-Aldrich; Merck KGaA) for *in vitro* assays.

Cell viability assay. Cell viability was evaluated using a CellTiter-Glo Luminescent Cell Viability Assay kit (cat. no. G7572; Promega Corporation) according to the manufacturer's instructions. Cells were treated with 10 μ g/ml propofol or equal volume of DMSO as control for the cell viability assay. In brief, the cells and CellTiter-Glo reagents were kept at room temperature for 30 min, then mixed thoroughly and incubated in a dark room for 10 min.

Then, the luminescence signal (400-700 nm) was recorded on a microplate reader (Multiskan SkyHigh; Thermo Fisher Scientific, Inc.). Each experiment was conducted in triplicate.

RNA extraction and reverse transcription-quantitative (RT-q) PCR. Total RNA from cell lines or tissue samples was extracted using TRIzol[®] reagent (Invitrogen; Thermo Fisher Scientific, Inc.) according to the manufacturer's instructions, then reverse transcribed into cDNA using a PrimeScript[™] RT kit (Takara Bio, Inc.), according to the manufacturer's protocol. qPCR was performed using SYBR Premix EX Taq[™] (Takara Bio, Inc.). Reaction conditions for qPCR were as follows: 95°C for 1 min; then 40 cycles of 95°C for 15 sec, 55°C for 30 sec and 72°C for 30 sec. The following primers were used: miR-145-5p forward, 5'-ACACTCCAGCTGGGAGTCT-3' and reverse, 5'-CTCAAC TGGTGTCTGTGGA-3'; TOP2A forward, 5'-GGGAGAGTG ATGACTTCCATATGGA-3' and reverse, 5'-AACACCTTC CCCAACTAAATTTCAG-3'; U6 forward, 5'-CGCTTCGGC AGCACATATACTA-3' and reverse, 5'-CGCTTCACGAAT TTGCGTGTCA-3'; and GAPDH forward, 5'-TGCACCACC AACTGCTTAGC-3' and reverse, 5'-GGCATGGACTGTGGT CATGAG-3'. U6 and GAPDH were used to normalize the expression of miRNA and mRNA, respectively, and results were analyzed via the 2^{- $\Delta\Delta C_q$} method (23).

Western blot analysis. Total protein was isolated using RIPA lysis buffer (Beijing Dingguo Changsheng Biotechnology Co., Ltd.) containing protease inhibitors (Beyotime Institute of Biotechnology). The protein concentration was determined using a BCA protein assay kit (Shanghai Zeye Biotechnology Co., Ltd.); then, 30 μ g protein was separated via 10% SDS-PAGE (Beyotime Institute of Biotechnology) and transferred onto PVDF membranes (Pall Life Sciences). The membranes were blocked with 5% skimmed milk at room temperature for 1 h, then incubated with the following primary antibodies at 4°C overnight: Anti-TOP2A (1:5,000; cat. no. ZY-6562-21R) and anti-GAPDH (1:2,000; cat. no. ZY-6909-37R; both Shanghai Zeye Biotechnology Co., Ltd.). The membranes were incubated with horseradish peroxidase-conjugated secondary antibody (1:4,000; cat. no. 98164; Cell Signaling Technology, Inc.) for 1 h at room temperature, then the hybridization signals were detected by Immobilon Western chemiluminescence (EMD Millipore) and captured using Amersham ImageQuant 600 imaging system (cat. no. 29083461; GE Healthcare). The semi-quantification of the western blots was conducted using ImageJ version 1.52 (National Institutes of Health).

Plasmids, lentiviral packaging and cell transfection. The miR-145-5p antisense oligonucleotide inhibitor (anti-miR-145-5p, 5'-AGGGA TTCCT GGGAA AACTG GAC-3', anti-miR-NC, 5'-ACGGA GGCTA AGCGT CGCAA-3') was purchased from Shanghai Shenggong Biology Engineering Technology Service, Ltd. TOP2A-specific small interfering (si)RNA was obtained from Santa Cruz Biotechnology, Inc., and the sequences were as follows: si-TOP2A, 5'-ACCTTTGACTCTCAGACAAAAGA-3' and si-NC, 5'-CCAGTTATGCTGACATGTAT-3'. The expression plasmid for miR-145-5p was constructed by cloning the mature

sequence (5'-GTCCAGTTTTCCCAGGAATCCCT-3') into a pCMV-MIR lentiviral vector (cat. no. PCMV-MIR; OriGene Technologies, Inc.). Empty pCMV-MIR lentiviral plasmid was used as an empty vector control (EV). Recombinant lentiviral particles were produced in 293T cells (American Type Culture Collection) via co-transfection with the helper plasmids pCMV-VSV-G, pRSV-REV and pMDL at a ratio of 5:1:5:5 using Lipofectamine® 3000 (Invitrogen; Thermo Fisher Scientific, Inc.). The virus-containing supernatant was harvested at 24, 48 and 72 h after transfection and filtered using 0.22- μ m filters, then stored at -80°C for further use. For viral infection, 500 μ l virus-containing supernatant was added to 1×10^5 cells with 8 μ g/ml polybrene overnight, then selected with puromycin (2 μ g/ml) for 72 h. For transient transfection, cells (1×10^6 cells) were seeded in 6-well plates and transfected with miR-145-5p mimics, anti-miR-145-5p or si-TOP2A using Lipofectamine 3000 (Invitrogen; Thermo Fisher Scientific, Inc.) according to the manufacturer's protocols. In brief, plasmids were mixed with Lipofectamine 3000 reagents and incubated with cells overnight, then used for further studies at 24 h post-transfection.

Database mining. Gene Expression Omnibus (GEO; <http://www.ncbi.nlm.nih.gov/gds/>) was used to identify differentially expressed genes between BC samples and matched normal tissues in the GSE76211 dataset (24). RNA sequencing data was aligned using PRADA tool (<https://www.rna-seqblog.com/prada-pipeline-for-rna-sequencing-data-analysis/>). The RNA-seq reads were counted over gene exons using HTSeq V0.6.1 (https://htseq.readthedocs.io/en/release_0.11.1/). DESeq R package (1.10.1) (<http://bioconductor.org/packages/release/bioc/html/DESeq.html>) was used to evaluate the differences between the samples. $P < 0.05$ and \log_2 fold-change ≥ 2 were used to select differentially expressed genes.

Dual-luciferase reporter assay. The targets of miR-145-5p were predicted using StarBase 2.0 (<http://starbase.sysu.edu.cn/index.php>). TargetScan 7.0 (<http://www.targetscan.org>) was used to identify potential binding sites between TOP2A and miR-145-5p. Cells (1×10^6 cells) were seeded in 6-well plates; then, the wild-type (WT) 3'-untranslated region (3'UTR) of the TOP2A containing the putative miR-145-5p binding sites or a mutant (MUT) sequence was inserted into a pMIR plasmid containing a firefly luciferase reporter prior to transfection with Lipofectamine 3000. 293T cells were co-transfected with pMIR plasmid containing the 3' UTR of WT TOP2A or MUT, miR-145-5p mimics or miR-NC, and a Renilla luciferase plasmid at a ratio of 2:2:1. After 48 h, the luciferase activity was detected using a dual-luciferase reporter assay system (Promega Corporation).

Wound healing assay. Cells were treated with 10 μ g/ml propofol or equal volume of DMSO as a control for the wound-healing assay. In brief, cells (2×10^5 cells) were seeded in a 12-well plate and cultured to full confluence. The cell monolayer was scratched along the center using a pipette tip and then washed three times with PBS to remove the detached cells. Cells were then cultured with 10% FBS (Cytiva; Hyclone) at 37°C in a humidified incubator containing 5% CO₂ (11). The wounds were observed with a microscope (Zeiss AG) at 0 and 24 h.

Transwell cell invasion assay. Cells were treated with 10 μ g/ml propofol or equal volume of DMSO as a control for the Transwell invasion assay. In brief, cells (1×10^4 /well) were suspended in serum-free medium and seeded in the upper chamber with 8- μ m pore filters (EMD Millipore). The filters were precoated with Matrigel (BD Biosciences) at room temperature for 24 h. The lower chamber was filled with complete medium. Following incubation for 24 h, invaded cells were fixed with 4% paraformaldehyde for 15 min at room temperature and stained with 0.5% crystal violet (Nanjing Jiancheng Bioengineering Institute) for 1 h at room temperature. The cells were observed with a microscope (Zeiss AG). For each sample, five fields of view were randomly selected.

Tumor xenograft model. The animal study was approved by the Ethics Committee of the University of Electronic Science and Technology of China. Six-week old BALB/C nude mice (25-30 g) were housed in individually ventilated cages under specific pathogen-free conditions at 25°C and 12 h light/dark cycle. Mice were allowed access to sterilized water and food *ad libitum*. First, T24 cells in the logarithmic phase were transfected with anti-miR-145-5p oligonucleotide inhibitor or anti-miR-negative control (NC), then injected subcutaneously into 15 female BALB/C nude mice (Shanghai Model Organisms Center, Inc.) 24 h post-transfection. Mice were randomly divided into 3 groups ($n=5$ /group): Vehicle + anti-miR-NC group; propofol + anti-miR-NC group; and propofol + anti-miR-145-5p group. The propofol + anti-miR-145-5p group was injected with T24 cells transfected with anti-miR-145-5p, then intraperitoneally injected with 10 mg/kg propofol. The propofol + anti-miR-NC group was injected with T24 cells transfected with anti-miR-145-5p, then treated with an equal volume of vehicle control (Soybean oil). The vehicle + anti-miR-NC group was injected with T24 cells transfected with anti-miR-NC, then treated with an equal volume of vehicle control. Propofol was intraperitoneally injected daily for 4 weeks. Tumor growth was measured via a two-dimensional measurement method and calculated as follows: $\text{Volume} = (A^2 \times B) / 2$, where A was the smallest diameter of the tumor and B was the largest diameter of the tumor. All mice were anesthetized via inhalation of 3% isoflurane and sacrificed via cervical dislocation at the end of the experiment.

Immunohistochemistry. Mouse xenograft samples were fixed in 10% formalin at room temperature overnight, embedded in paraffin and cut into 3- μ m sections. Endogenous peroxidase activity was blocked with 3% H₂O₂ at room temperature for 15 min. Antigen retrieval was performed in citrate buffer and sections were washed with PBS. Then, sections were subsequently blocked with 1% bovine serum albumin (Sigma-Aldrich; Merck KGaA) for 1 h at room temperature. Next, the sections were incubated with primary antibodies against E-cadherin (1:200; cat. no. 3195; Cell Signaling Technology, Inc.) or vimentin (1:200; cat. no. ab92547; Abcam) at 4°C overnight and the biotin-conjugated secondary antibody (1:3,000; cat. no. 14708; Cell Signaling Technology, Inc.) at room temperature for 10 min. Streptavidin-peroxidase was applied for 15 min at room temperature followed by development

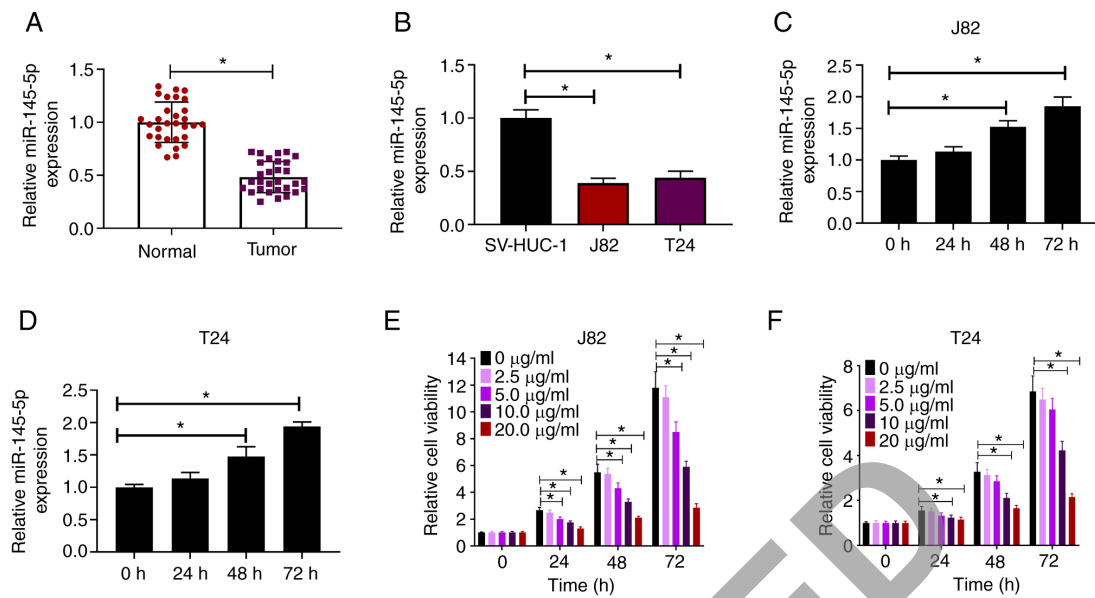


Figure 1. Propofol induces miR-145-5p expression in BC cells. (A) Relative expression of miR-145-5p in 30 BC samples and paired normal tissues as determined via RT-qPCR. (B) Relative expression of miR-145-5p in BC cell lines (J82 and T24) and SV-HUC-1 cells as determined via RT-qPCR. Relative expression of miR-145-5p in (C) J82 and (D) T24 cells at different time points after exposure to 10 $\mu\text{g/ml}$ propofol. (E) J82 and (F) T24 cells were treated with increasing concentrations (0–20 $\mu\text{g/ml}$) of propofol for 24, 48 or 72 h, then cell viability was evaluated. Each assay was performed in triplicate and data are presented as the mean \pm SD. * $P < 0.05$. BC, breast cancer; miR, microRNA; RT-qPCR, reverse transcription-quantitative PCR.

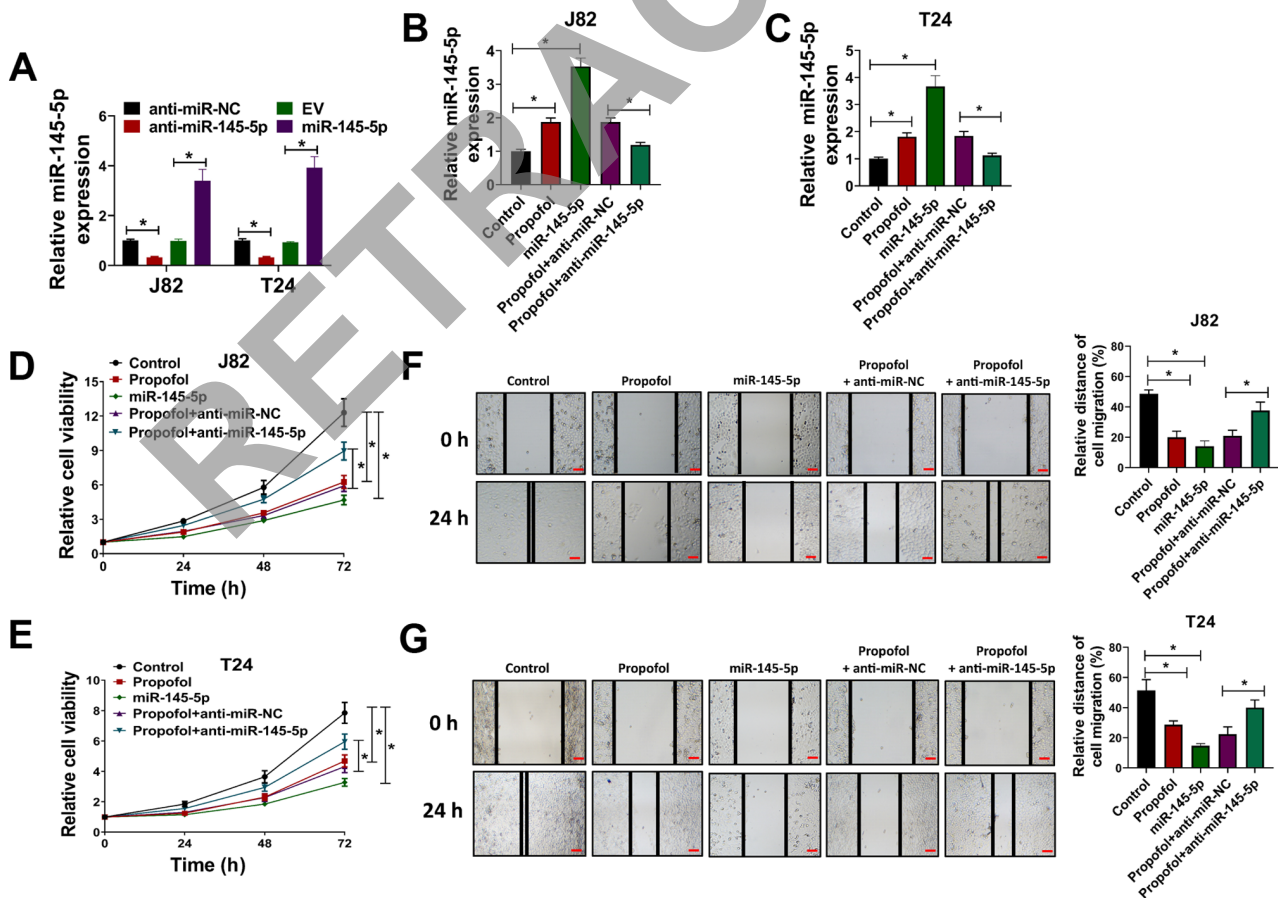


Figure 2. Propofol inhibits the proliferation and migration of bladder cancer cells by regulating miR-145-5p expression. (A) J82 and T24 cells were transfected with anti-miR-145-5p, anti-miR-NC, EV or miR-145-5p, then the relative expression of miR-145-5p was evaluated via RT-qPCR. (B) J82 and (C) T24 cells were transfected with anti-miR-145-5p, anti-miR-NC or miR-145-5p and exposed to 10 $\mu\text{g/ml}$ propofol, then relative miR-145-5p expression was evaluated via RT-qPCR. (D) J82 and (E) T24 cells were transfected with anti-miR-145-5p, anti-miR-NC or miR-145-5p and exposed to 10 $\mu\text{g/ml}$ propofol, then cell viability was evaluated at 24, 48 and 72 h post-drug treatment. (F) J82 and (G) T24 cells were transfected with anti-miR-145-5p, anti-miR-NC or miR-145-5p and exposed to 10 $\mu\text{g/ml}$ propofol, then cells were used for wound-healing assays. Scale bar, 500 μm . Each assay was performed in triplicate and data are presented as the mean \pm SD. * $P < 0.05$. miR, microRNA; NC, negative control; EV, empty vector; RT-qPCR, reverse transcription-quantitative PCR.

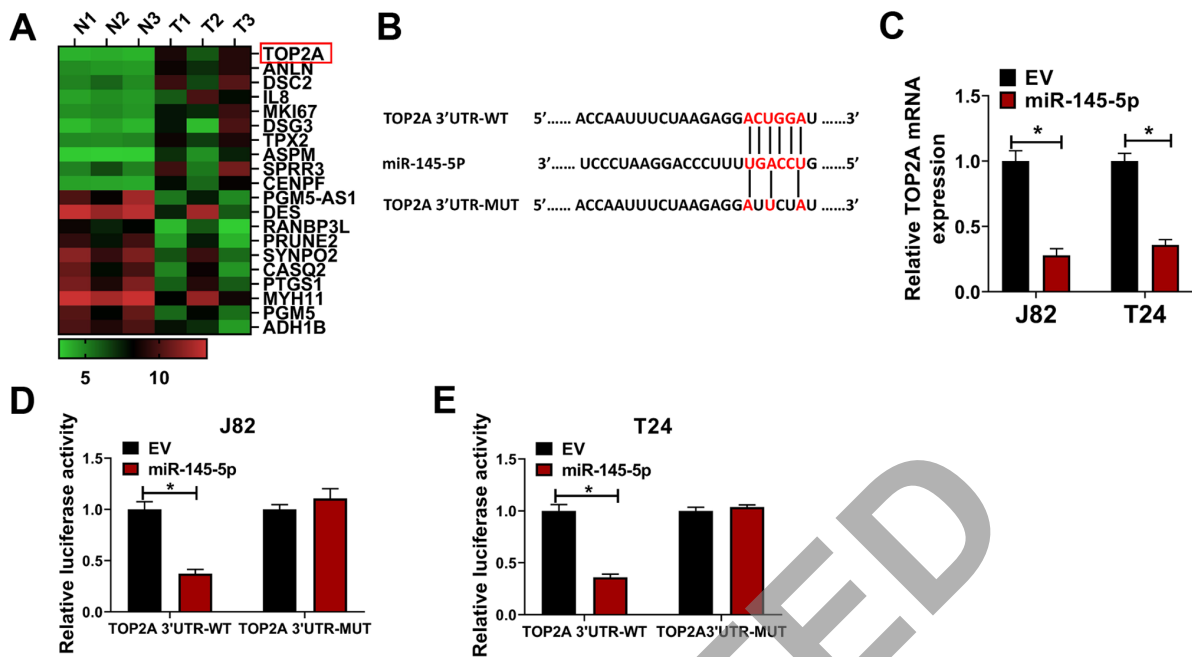


Figure 3. Identification of TOP2A as a target of miR-145-5p. (A) Top 10 mRNA transcripts upregulated and downregulated in GSE76211 are shown in a heat map. (B) Potential binding site for TOP2A and miR-145-5p as identified by TargetScan. (C) J82 and T24 cells were transduced with miR-145-5p or EV lentivirus control, then relative TOP2A expression was evaluated via reverse transcription-quantitative PCR. (D) J82 and (E) T24 cells were transfected with EV or miR-145-5p and TOP2A 3'UTR-WT or TOP2A 3'UTR-MUT, then cells were used for luciferase reporter assays. Each assay was performed in triplicate and data are presented as the mean \pm SD. * $P < 0.05$. N, normal; T, tumor; miR, microRNA; EV, empty vector; TOP2A, topoisomerase II α ; 3'UTR, 3-untranslated region; WT, wild-type; MUT, mutant.

with DAB. Then, the sections were counterstained with Mayer's Hematoxylin for 2 min at room temperature. Subsequently, the sections were dehydrated and sealed with neutral gum. Images were photographed using the LSM 5 Pa Laser Scanning Microscope (Zeiss AG).

Statistical analysis. SPSS 20.0 software (IBM Corp.) was used to perform statistical analysis. All experiments were repeated at least three times and data were presented as the mean \pm SD. Comparisons between two different groups were performed using independent-samples t-tests or paired t-tests, and comparisons of multiple groups were performed using one-way ANOVA with Bonferroni's post hoc test. The correlation between miR-145-5p and TOP2A mRNA was evaluated using Spearman's correlation analysis. $P < 0.05$ was considered to indicate a statistically significant difference.

Results

Propofol induces miR-145-5p expression in BC cells. The expression of miR-145-5p in BC samples and cell lines was measured via RT-qPCR. Compared with paired normal tissues, miR-145-5p expression was significantly downregulated in BC tissues (Fig. 1A). Similarly, miR-145-5p was downregulated in human BC cell lines (J82 and T24) compared with the human uroepithelial SV-HUC-1 cell line (Fig. 1B). To explore the effects of propofol on miR-145-5p expression, J82 and T24 cells were treated with propofol and evaluated for miR-145-5p expression at different time points. It was found that miR-145-5p expression was induced by propofol in both J82 and T24 cells in a time-dependent

manner (Fig. 1C and D). J82 and T24 cells were exposed to increasing concentrations of propofol (0-20 μ g/ml) for 24, 48 and 72 h, then cell viability was evaluated. It was found that propofol reduced the viability of BC cells in a dose-dependent manner (Fig. 1E and F). Collectively, these findings indicated that propofol induced miR-145-5p expression in BC cells.

Propofol suppresses cell proliferation, migration and invasion by regulating miR-145-5p. To study the effects of propofol in BC cells and whether its biological effects were associated with miR-145-5p expression, J82 and T24 cells were transfected with miR-145-5p lentivirus or anti-miR-145-5p oligonucleotides, then exposed to propofol for cell viability, wound-healing and Transwell cell invasion assays. The expression of miR-145-5p in J82 and T24 cells was significantly downregulated via transfection with anti-miR-145-5p and upregulated via transfection with miR-145-5p, compared with the respective negative controls (Fig. 2A). Then, J82 and T24 cells transfected with miR-145-5p or anti-miR-145-5p were exposed to propofol, and the expression of miR-145-5p was evaluated via RT-qPCR. It was observed that propofol-induced miR-145-5p expression in J82 and T24 cells was attenuated by transduction with anti-miR-145-5p (Fig. 2B and C). In a cell viability assay, it was observed that propofol treatment or miR-145-5p overexpression decreased the viability of J82 and T24 cells, while anti-miR-145-5p reversed the effects induced by propofol treatment (Fig. 2D and E). Wound-healing assays demonstrated that cell migration was significantly reduced when J82 or T24 cells were

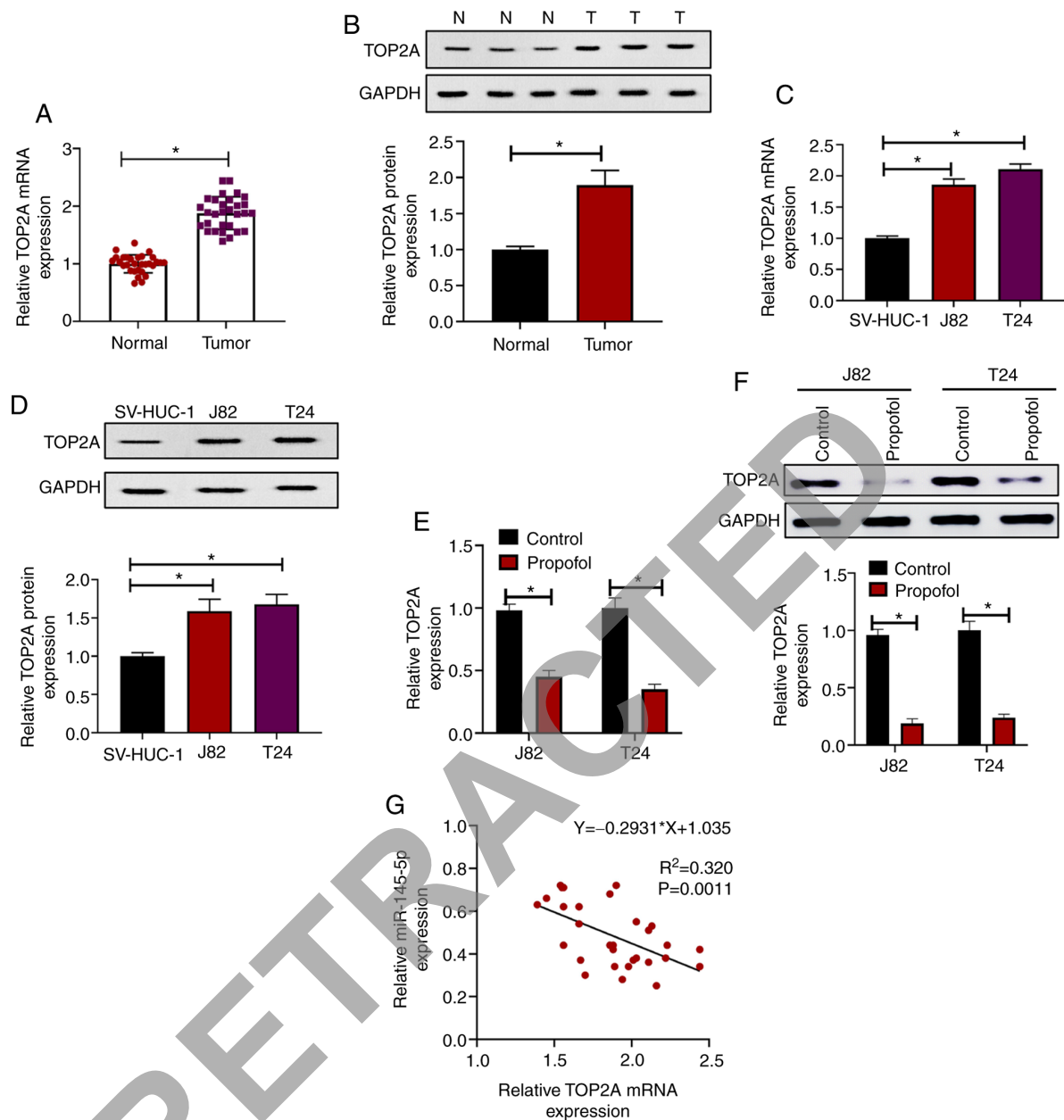


Figure 4. Propofol suppresses TOP2A expression in BC cells. (A) Relative TOP2A expression in 30 BC samples and paired normal tissues as determined via RT-qPCR. (B) Relative TOP2A expression between BC samples and paired normal tissues as determined via western blot analysis. (C) Relative TOP2A expression in different cell lines as determined via RT-qPCR. (D) Relative TOP2A expression in different cell lines as determined via western blot analysis. J82 and T24 cells were treated with 10 μ g/ml propofol or an equal volume of DMSO as control, then relative TOP2A expression was evaluated via (E) RT-qPCR and (F) western blot analysis. (G) Spearman correlation analysis of miR-145-5p and TOP2A expression in patients with BC. Each assay was performed in triplicate and data are presented as the mean \pm SD. * $P < 0.05$. BC, bladder cancer; N, normal; T, tumor; miR, microRNA; TOP2A, topoisomerase II α ; RT-qPCR, reverse transcription-quantitative PCR.

treated with propofol or transduced with miR-145-5p compared with the vehicle control group (equal volume of DMSO). As expected, the extent of wound closure was significantly increased in the propofol + anti-miR-145-5p group compared with the propofol + anti-miR-NC group (Fig. 2F and G), indicating that propofol reduced the migration of BC cells by promoting miR-145-5p expression. In Transwell cell invasion assays, propofol treatment and miR-145-5p overexpression significantly decreased the number of invading cells compared with the control group, while depletion of miR-145-5p via transduction with anti-miR-145-5p attenuated the effects induced by propofol

treatment (Fig. S1A and B). Collectively, the results indicated that propofol suppressed the proliferation, migration and invasion of BC cells, and that this effect was partially mediated by regulating miR-145-5p expression.

Identification of TOP2A as direct target of miR-145-5p in BC cells. The top 10 upregulated and downregulated mRNA molecules in the GSE76211 from the GEO were screened and are shown in a heat map (Fig. 3A). TOP2A (\log_2 fold-change=4.5; $P < 0.001$) was the most affected mRNA among the 20 targeted mRNAs; thus, it was hypothesized that TOP2A may be a direct target of miR-145-5p.

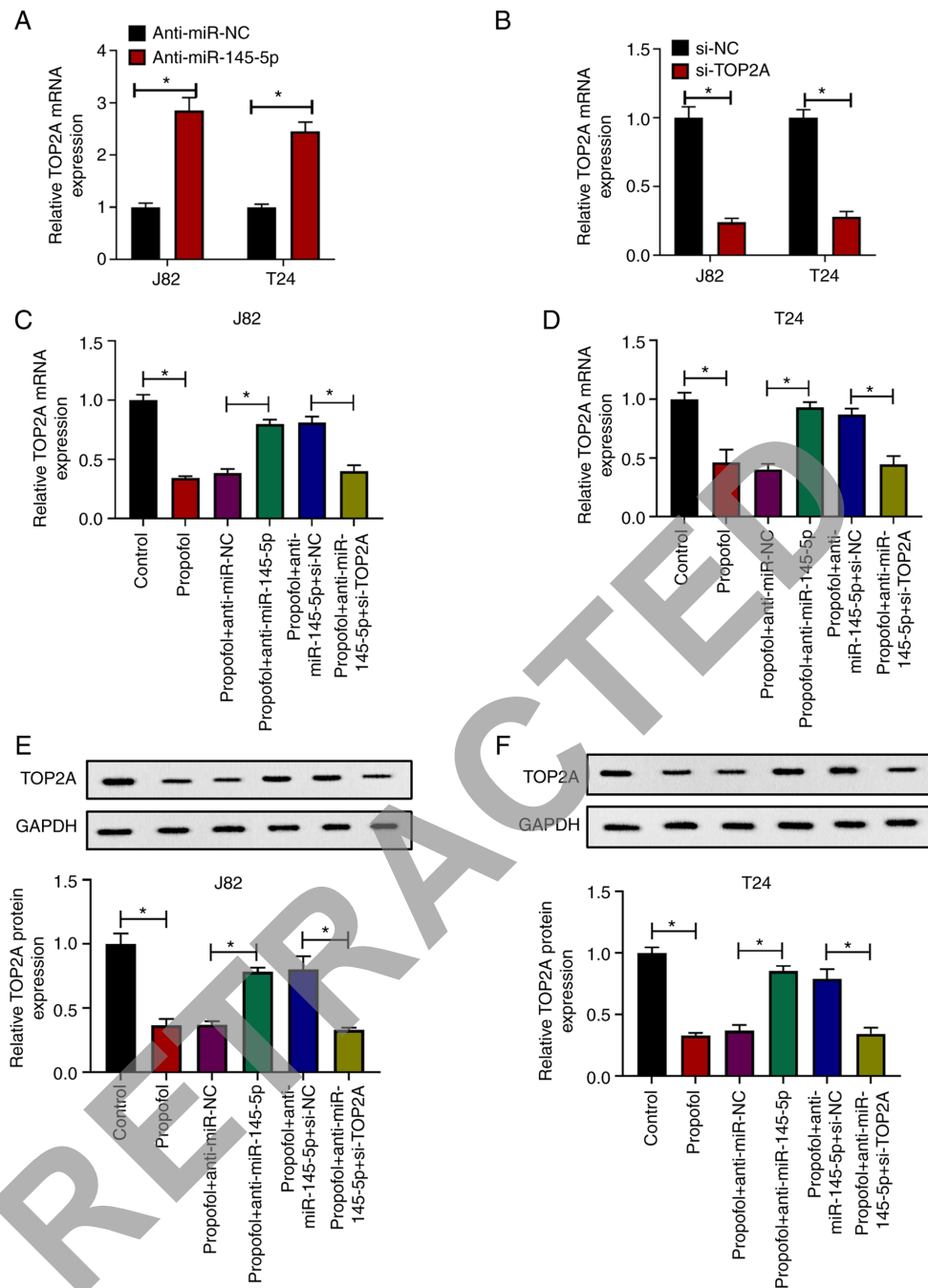


Figure 5. Propofol exerts antitumor effects via the miR-145-5p/TOP2A axis. (A) J82 and T24 cells were transduced with anti-miR-NC or anti-miR-145-5p, then relative TOP2A expression was evaluated via RT-qPCR. (B) J82 and T24 cells were transfected with si-NC or si-TOP2A, then relative TOP2A expression was evaluated via RT-qPCR. (C) J82 and (D) T24 cells were transduced with anti-miR-NC, anti-miR-145-5p, si-NC or si-TOP2A, then treated with 10 μ g/ml propofol or an equal volume of DMSO as control. Relative TOP2A expression was evaluated via RT-qPCR. (E) J82 and (F) T24 cells were transduced with anti-miR-NC, anti-miR-145-5p, si-NC or si-TOP2A, then treated with 10 μ g/ml propofol or an equal volume of DMSO as control. Relative TOP2A expression was evaluated via western blotting. Each assay was performed in triplicate and data are presented as the mean \pm SD. * P <0.05. miR, microRNA; si, small interfering RNA; NC, negative control; TOP2A, topoisomerase II α ; RT-qPCR, reverse transcription-quantitative PCR.

TargetScan 7.0 was used to identify potential binding sites between TOP2A and miR-145-5p (Fig. 3B). To reveal the direct effect of miR-145-5p on TOP2A, miR-145-5p was overexpressed in J82 and T24 cells, and TOP2A expression was evaluated. It was found that the mRNA expression of TOP2A was significantly downregulated following miR-145-5p overexpression (Fig. 3C). In luciferase reporter assays, the luciferase activity was significantly reduced by co-transfection of miR-145-5p + TOP2A 3'UTR-WT

compared with the control, whereas the luciferase activity in cells co-transfected with miR-145-5p + TOP2A 3'UTR-MUT was not significantly altered (Fig. 3D and E). The expression of TOP2A was evaluated in BC samples and paired normal tissues, and it was found that both the mRNA (Fig. 4A) and protein expression levels (Fig. 4B) of TOP2A were significantly upregulated in tumor samples compared with paired normal tissues. Consistent with this, it was revealed that TOP2A mRNA (Fig. 4C) and protein (Fig. 4D) expression

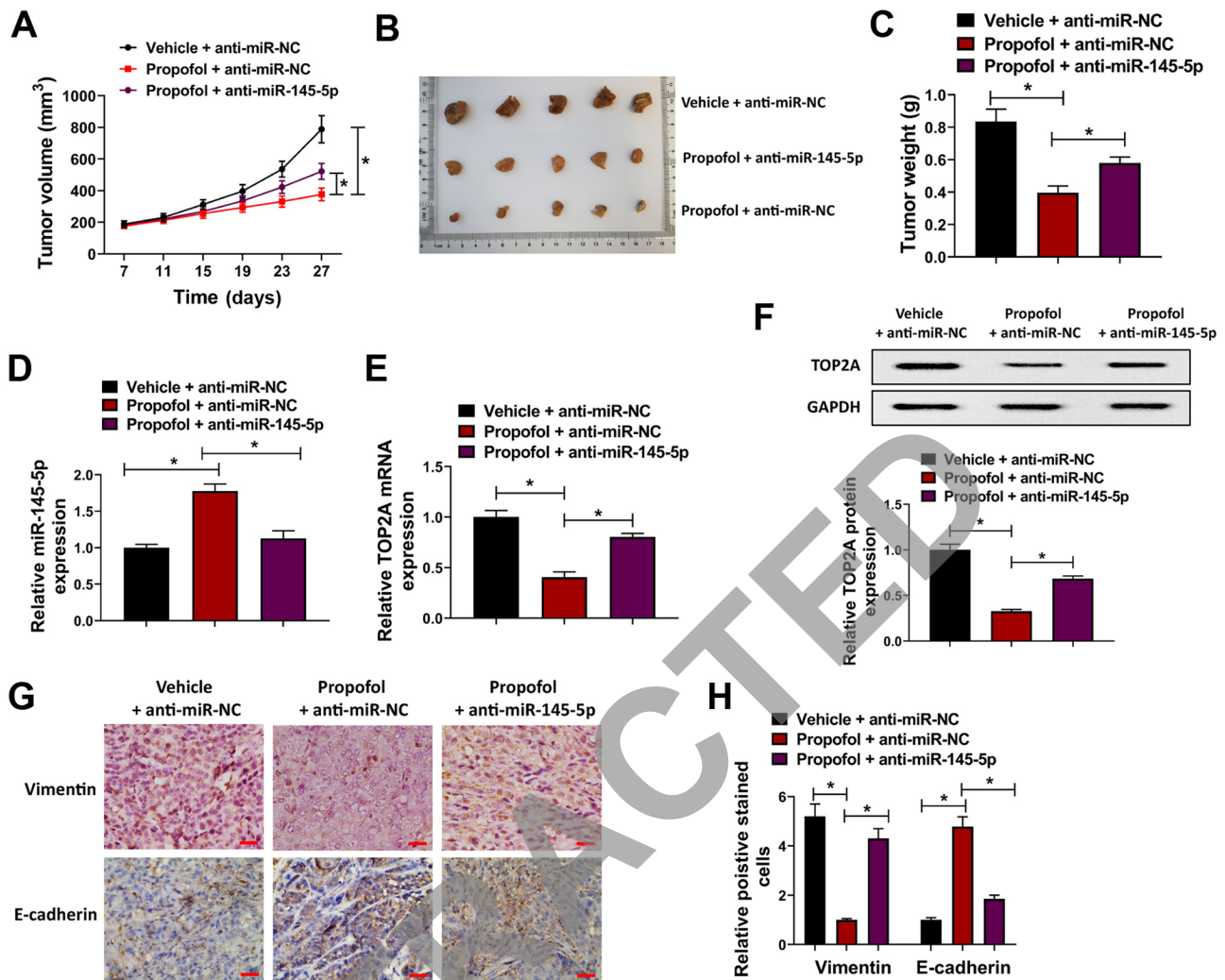


Figure 6. Propofol attenuates tumor growth via regulation of miR-145-5p/TOP2A *in vivo*. T24 cells were transduced with anti-miR-145-5p or anti-miR-NC lentiviral vectors and then injected into female BALB/C nude mice, which were treated with 10 mg/kg propofol for 4 weeks. (A) Tumor growth curves, (B) images of tumors and (C) tumor weights in each group. (D) Relative tumor miR-145-5p expression in different groups as determined via RT-qPCR. Relative tumor TOP2A expression in different groups as determined via (E) RT-qPCR or (F) western blotting. (G) Expression of vimentin and E-cadherin in tumor xenografts from each group was detected via immunohistochemistry; (H) relative numbers of positively stained cells were shown. Scale bar, 500 μ m. Each assay was performed in triplicate and data are presented as the mean \pm SD. * P <0.05. miR, microRNA; NC, negative control; TOP2A, topoisomerase II α ; RT-qPCR, reverse transcription-quantitative PCR.

was increased in J82 and T24 cells compared with SV-HUC-1 cells. In addition, it was observed that when treated with propofol for 72 h, the mRNA (Fig. 4E) and protein (Fig. 4F) levels of TOP2A were significantly reduced compared with the control, indicating that propofol inhibited the expression of TOP2A. Furthermore, correlation analysis of miR-145-5p and TOP2A mRNA expression in BC samples revealed that miR-145-5p and TOP2A were significantly negatively correlated ($P=-0.835$; $P=0.0011$; Fig. 4G). Collectively, these results indicated that TOP2A was directly targeted by miR-145-5p in BC cells.

Propofol exerts antitumor effects via the miR-145-5p/TOP2A axis. To investigate whether the antitumor effects of propofol were associated with the miR-145-5p/TOP2A axis, TOP2A expression was knocked down by transfecting J82 and T24 cells with anti-miR-145-5p or si-TOP2A. It was demonstrated that TOP2A expression was increased in J82 and T24 cells

transduced with anti-miR-145-5p compared with anti-miR-NC (Fig. 5A), while cells transfected with si-TOP2A exhibited downregulated expression of TOP2A compared with si-NC (Fig. 5B). Then, cells were transfected with anti-miR-NC, anti-miR-15-5p, si-NC or si-TOP2A as indicated, and then exposed to propofol. It was revealed that the mRNA (Fig. 5C and D) or protein expression levels (Fig. 5E and F) of TOP2A in J82 and T24 cells were suppressed by propofol treatment, and that this effect in propofol-treated cells was attenuated by anti-miR-145-5p, which was again reversed by si-TOP2A transfection, compared with the corresponding negative controls. In wound-healing (Fig. S2A and B) and Transwell assays (Fig. S2C and D), propofol suppressed the migration and invasion of J82 and T24 cells, which was partially attenuated by anti-miR-145-5p and further exacerbated by subsequent TOP2A knockdown. Taken together, these results indicated that propofol exerted antitumor effects via the miR-145-5p/TOP2A axis.

Propofol attenuates tumor growth by regulating the miR-145-5p/TOP2A axis in vivo. In order to further verify the antitumor effect of propofol *in vivo*, a BC cell xenograft nude mouse model was constructed. T24 cells were transfected with anti-miR-145-5p lentiviral vectors or anti-miR-NC, and then injected into female BALB/C nude mice prior to treatment with 10 mg/kg propofol for 4 weeks. It was revealed that tumor volume and weight were significantly decreased in the propofol + anti-miR-NC group compared with the vehicle + anti-miR-NC group, whereas this effect was attenuated in the propofol + anti-miR-145-5p group, indicating that propofol suppressed the proliferation of BC cells, which was partially attenuated by miR-145-5p knockdown (Fig. 6A-C). Moreover, the expression of miR-145-5p was upregulated by propofol and downregulated by anti-miR-145-5p in tumor tissues (Fig. 6D). Conversely, the mRNA and protein expression levels of TOP2A were suppressed by propofol; this effect was attenuated by anti-miR-145-5p (Fig. 6E and F). The expression of E-cadherin and vimentin was investigated in tumor xenograft tissues from the different groups, and it was revealed that E-cadherin expression was increased, while that of vimentin was downregulated, by propofol, and that these effects were attenuated by anti-miR-145-5p (Fig. 6G and H). Collectively, these findings indicated that propofol suppressed tumor growth by regulating the miR-145-5p/TOP2A axis *in vivo*.

Discussion

Anesthesia is an important medical process during cancer resection, and propofol is one of the most commonly used anesthetics (7). The effects of propofol in patients with cancer are controversial, as *in vitro* experiments have reported diverse effects. Garib *et al* (25) reported that propofol increased the migration of breast cancer cells; however, Miao *et al* (26) suggested that propofol inhibited the invasion of colon cancer cells. Qi *et al* (27) revealed a tumor-suppressive effect of propofol in BC by suppressing cell proliferation, migration and invasion. In the present study, it was revealed that propofol inhibited the viability, migration and invasion of BC cells *in vitro*, and suppressed tumor xenograft growth *in vivo*; this was consistent with previous reports that propofol exhibits antitumor effects.

There is increasing evidence indicating that propofol exerts antitumor effects by regulating miRNA. For example, in gastric cancer, propofol was reported to suppress the proliferation, migration and invasion of MKN45 cells by upregulating miR-195 (28). In lung cancer, propofol suppressed cell proliferation and the epithelial-mesenchymal transition (EMT) process by upregulating miR-1284 (29). Conversely, another study showed that propofol inhibited the adhesion of A549 cells by downregulating miR-372 (30). Distinct effects of propofol have been observed in different types of cancer cell. In a clinical study, propofol anesthesia was suggested to increase the disease-free survival of patients with BC (31). In the present study, it was found that propofol significantly inhibited cell proliferation, migration and invasion, which was consistent with previous reports.

Accumulating studies indicate that miR-145-5p serves an important role in the tumorigenesis and progression of a number of cancers, such as ovarian (32), colon (33) and prostate cancers (34). In BC, miR-145 was reported to be a diagnostic marker that was downregulated in BC samples (13-15). Furthermore, miR-145 was found to suppress the proliferation and migration of BC cells by targeting transgelin-2 (35). Zhu *et al* (36) also found that miR-145 directly targeted the proto-oncogene insulin-like growth factor 1 receptor, and suppressed the proliferation and induced the apoptosis of BC cells. Fujii *et al* (37) reported that miR-145 overexpression may induce cell senescence, inhibit cell proliferation and promote cell differentiation in urothelial carcinoma cells. These studies indicated that miR-145 acts as a tumor suppressor and exhibits diverse functions in BC. In the present study, it was observed that propofol induced miR-145 expression in BC cells, while knockdown of miR-145-5p partially reversed the effects of propofol, indicating that miR-145-5p was important for the antitumor effects of propofol in BC.

In the present study, TOP2A was identified as a potential target gene of miR-145-5p. As a topoisomerase, TOP2A serves an important role in cell division (22). Previous studies reported that aberrant TOP2A expression promotes tumor growth, metastasis and chemotherapeutic drug resistance by regulating DNA topological states (38,39). In the present study, an inverse correlation was observed between TOP2A and miR-145-5p in BC tissues. Although propofol suppressed the expression of TOP2A, this effect was significantly reversed by miR-145-5p knockdown. These results suggested that propofol exerted antitumor effects via the miR-145-5p/TOP2A axis. An *in vivo* tumor xenograft study revealed similar effects on miR-145-5p and TOP2A expression levels. Vimentin is a mesenchymal cell marker and E-cadherin is an epithelial cell marker (40). It was observed that E-cadherin expression was increased in propofol-treated mice, while vimentin was downregulated; these effects were attenuated by anti-miR-145-5p, indicating that propofol suppressed the EMT of BC cells. Pei *et al* (21) reported that TOP2A induced EMT and cell metastasis in pancreatic cancer by directly interacting with β -catenin. There were some limitations of the present study. For example, subsequent experiments were not conducted in the present study to identify the possible role of propofol in EMT, thus it is hypothesized that this was due to suppression of TOP2A expression in BC cells. Furthermore, this study used a high concentration of propofol and 10% FBS was used in the wound healing assay, which may have altered the results of the migration assay.

In summary, the present study revealed that propofol suppressed the proliferation, migration and invasion of BC cells *in vitro* and xenograft growth *in vivo* via the miR-145-5p/TOP2A axis. These findings provided novel insight into the potential advantages of using propofol anesthesia during BC surgery.

Acknowledgements

Not applicable.

Funding

No funding was received.

Availability of data and materials

The datasets used and/or analyzed during the current study are available from the corresponding author on reasonable request.

Authors' contributions

HZ guaranteed the integrity of the entire study. The experiments were conducted by YD, XZ, HZ and YC. Clinical studies were conducted by SZ and JS. Data were analyzed by HP. The manuscript was prepared and reviewed by HZ and YD. YD, XZ, HZ and YC confirm the authenticity of all the raw data. All authors read and approved the final manuscript.

Ethics approval and consent to participate

For the patient study, all samples were obtained after receiving informed consent from patients, and the study protocol was approved by the Ethics Committee of the University of Electronic Science and Technology of China (Chengdu, China). The animal study was approved by the Ethics Committee of the University of Electronic Science and Technology of China.

Patient consent for publication

Not applicable.

Competing interests

The authors declare that they have no competing interests.

References

- Knowles MA and Hurst CD: Molecular biology of bladder cancer: New insights into pathogenesis and clinical diversity. *Nat Rev Cancer* 15: 25-41, 2015.
- Polo A, Crispo A, Cerino P, Falzone L, Candido S, Giudice A, De Petro G, Ciliberto G, Montella M, Budillon A and Costantini S: Environment and bladder cancer: Molecular analysis by interaction networks. *Oncotarget* 8: 65240-65252, 2017.
- Cumberbatch MGK and Noon AP: Epidemiology, aetiology and screening of bladder cancer. *Transl Androl Urol* 8: 5-11, 2019.
- Alfred Witjes J, Lebre T, Compérat EM, Cowan NC, De Santis M, Bruins HM, Hernández V, Espinós EL, Dunn J, Rouanne M, *et al*: Updated 2016 EAU guidelines on muscle-invasive and metastatic bladder cancer. *Eur Urol* 71: 462-475, 2017.
- Falzone L, Salomone S and Libra M: Evolution of cancer pharmacological treatments at the turn of the third millennium. *Front Pharmacol* 9: 1300, 2018.
- Kim R: Effects of surgery and anesthetic choice on immunosuppression and cancer recurrence. *J Transl Med* 16: 8, 2018.
- Zheng X, Wang Y, Dong L, Zhao S, Wang L, Chen H, Xu Y and Wang G: Effects of propofol-based total intravenous anesthesia on gastric cancer: A retrospective study. *Onco Targets Ther* 11: 1141-1148, 2018.
- Wigmore TJ, Mohammed K and Jhanji S: Long-term survival for patients undergoing volatile versus IV anesthesia for cancer surgery. *Anesthesiology* 124: 69-79, 2016.
- Du Q, Liu J, Zhang X, Zhang X, Zhu H, Wei M and Wang S: Propofol inhibits proliferation, migration, and invasion but promotes apoptosis by regulation of Sox4 in endometrial cancer cells. *Br J Med Biol Res* 51: e6803, 2018.
- Zhang J, Zhang D, Wu GQ, Feng ZY and Zhu SM: Propofol inhibits the adhesion of hepatocellular carcinoma cells by upregulating microRNA-199a and downregulating MMP-9 expression. *Hepatobiliary Pancreat Dis Int* 12: 305-309, 2013.
- Zhang L, Wang N, Zhou S, Ye W, Jing G and Zhang M: Propofol induces proliferation and invasion of gallbladder cancer cells through activation of Nrf2. *J Exp Clin Cancer Res* 31: 66, 2012.
- Li Q, Wang H, Peng H, Huang Q, Huan T, Huang Q, Yang H and Shi J: MicroRNAs: Key players in bladder cancer. *Mol Diagn Ther* 23: 579-601, 2019.
- Dyrskjot L, Ostensfeld MS, Bramsen JB, Silahatoglu AN, Lamy P, Ramanathan R, Fristrup N, Jensen JL, Andersen CL, Zieger K, *et al*: Genomic profiling of microRNAs in bladder cancer: MiR-129 is associated with poor outcome and promotes cell death in vitro. *Cancer Res* 69: 4851-4860, 2009.
- Dip N, Reis ST, Srougi M, Dall'Oglio MF and Leite KR: Expression profile of microRNA-145 in urothelial bladder cancer. *Int Braz J Urol* 39: 95-102, 2013.
- Pignot G, Cizeron-Clairac G, Vacher S, Susini A, Tozlu S, Vieillefond A, Zerbib M, Lidereau R, Debre B, Amsellem-Ouazana D and Bieche I: microRNA expression profile in a large series of bladder tumors: Identification of a 3-miRNA signature associated with aggressiveness of muscle-invasive bladder cancer. *Int J Cancer* 132: 2479-2491, 2013.
- Minami K, Taniguchi K, Sugito N, Kuranaga Y, Inamoto T, Takahara K, Takai T, Yoshikawa Y, Kiyama S, Akao Y and Azuma H: MiR-145 negatively regulates Warburg effect by silencing KLF4 and PTBP1 in bladder cancer cells. *Oncotarget* 8: 33064-33077, 2017.
- Blick C, Ramachandran A, McCormick R, Wigfield S, Cranston D, Catto J and Harris AL: Identification of a hypoxia-regulated miRNA signature in bladder cancer and a role for miR-145 in hypoxia-dependent apoptosis. *Br J Cancer* 113: 634-644, 2015.
- Chiyomaru T, Enokida H, Tatarano S, Kawahara K, Uchida Y, Nishiyama K, Fujimura L, Kikkawa N, Seki N and Nakagawa M: miR-145 and miR-133a function as tumour suppressors and directly regulate FSCN1 expression in bladder cancer. *Br J Cancer* 102: 883-891, 2010.
- Wu KZ, Wang GN, Fitzgerald J, Quachthithu H, Rainey MD, Cattaneo A, Bachi A and Santocanale C: DDK dependent regulation of TOP2A at centromeres revealed by a chemical genetics approach. *Nucleic Acids Res* 44: 8786-8798, 2016.
- Zhang R, Xu J, Zhao J and Bai JH: Proliferation and invasion of colon cancer cells are suppressed by knockdown of TOP2A. *J Cell Biochem* 119: 7256-7263, 2018.
- Pei YF, Yin XM and Liu XQ: TOP2A induces malignant character of pancreatic cancer through activating β -catenin signaling pathway. *Biochim Biophys Acta Mol Basis Dis* 1864: 197-207, 2018.
- Slamon DJ and Press MF: Alterations in the TOP2A and HER2 genes: Association with adjuvant anthracycline sensitivity in human breast cancers. *J Natl Cancer Inst* 101: 615-618, 2009.
- Micael Reis CPV, Morales-Hojas R, Aguiar B, Rocha H, Schlötterer C and Vieira J: Fold change in regucalcin expression after chill-coma recovery (ChCR) obtained by qRT-PCR using the $2^{-\Delta\Delta Ct}$ method. *PLoS One* 6: e25520, 2011.
- Cao R, Meng Z, Liu T, Wang G, Qian G, Cao T, Guan X, Dan H, Xiao Y and Wang X: Decreased TRPM7 inhibits activities and induces apoptosis of bladder cancer cells via ERK1/2 pathway. *Oncotarget* 7: 72941-72960, 2016.
- Garib V, Lang K, Niggemann B, Zänker KS, Brandt L and Dittmar T: Propofol-induced calcium signalling and actin reorganization within breast carcinoma cells. *Eur J Anaesthesiol* 22: 609-615, 2005.
- Miao Y, Zhang Y, Wan H, Chen L and Wang F: GABA-receptor agonist, propofol inhibits invasion of colon carcinoma cells. *Biomed Pharmacother* 64: 583-588, 2010.
- Qi Z, Yuan L and Sun N: Propofol exhibits a tumor-suppressive effect and regulates cell viability, migration and invasion in bladder carcinoma by targeting the microRNA-10b/HOXD10 signaling pathway. *Oncol Lett* 18: 6228-6236, 2019.
- Zhang W, Wang Y, Zhu Z, Zheng Y and Song B: Propofol inhibits proliferation, migration and invasion of gastric cancer cells by up-regulating microRNA-195. *Int J Biol Macromol* 120: 975-984, 2018.
- Liu WZ and Liu N: Propofol inhibits lung cancer A549 cell growth and epithelial-mesenchymal transition process by upregulation of MicroRNA-1284. *Oncol Res* 27: 1-8, 2018.
- Sun H and Gao D: Propofol suppresses growth, migration and invasion of A549 cells by down-regulation of miR-372. *BMC Cancer* 18: 1252, 2018.

31. Guerrero Orriach JL, Raigon Ponferrada A, Malo Manso A, Herrera Imbroda B, Escalona Belmonte JJ, Ramirez Aliaga M, Ramirez Fernandez A, Diaz Crespo J, Soriano Perez AM, Fontaneda Heredia A, *et al*: Anesthesia in combination with propofol increases disease-free survival in bladder cancer patients who undergo radical tumor cystectomy as compared to inhalational anesthetics and opiate-based analgesia. *Oncology* 98: 161-167, 2020.
32. Hang W, Feng Y, Sang Z, Yang Y, Zhu Y, Huang Q and Xi X: Downregulation of miR-145-5p in cancer cells and their derived exosomes may contribute to the development of ovarian cancer by targeting CT. *Int J Mol Med* 43: 256-266, 2019.
33. Thüringer D, Jego G, Berthenet K, Hammann A, Solary E and Garrido C: Gap junction-mediated transfer of miR-145-5p from microvascular endothelial cells to colon cancer cells inhibits angiogenesis. *Oncotarget* 7: 28160-28168, 2016.
34. Xue D, Lu H, Xu HY, Zhou CX and He XZ: Long noncoding RNA MALAT1 enhances the docetaxel resistance of prostate cancer cells via miR-145-5p-mediated regulation of AKAP12. *J Cell Mol Med* 22: 3223-3237, 2018.
35. Zhang H, Jiang M, Liu Q, Han Z, Zhao Y and Ji S: miR-145-5p inhibits the proliferation and migration of bladder cancer cells by targeting TAGLN2. *Oncol Lett* 16: 6355-6360, 2018.
36. Zhu Z, Xu T, Wang L, Wang X, Zhong S, Xu C and Shen Z: MicroRNA-145 directly targets the insulin-like growth factor receptor I in human bladder cancer cells. *FEBS Lett* 588: 3180-3185, 2014.
37. Fujii T, Shimada K, Tatsumi Y, Hatakeyama K, Obayashi C, Fujimoto K and Konishi N: microRNA-145 promotes differentiation in human urothelial carcinoma through down-regulation of syndecan-1. *BMC Cancer* 15: 818, 2015.
38. Deng S, Yan T, Nikolova T, Fuhrmann D, Nemecek A, Gödtel-Armbrust U, Kaina B and Wojnowski L: The catalytic topoisomerase II inhibitor dexrazoxane induces DNA breaks, ATF3 and the DNA damage response in cancer cells. *Br J Pharmacol* 172: 2246-2257, 2015.
39. Chen T, Sun Y, Ji P, Kopetz S and Zhang W: Topoisomerase II α in chromosome instability and personalized cancer therapy. *Oncogene* 34: 4019-4031, 2014.
40. Wang Y, Zhao Y, Herbst A, Kalinski T, Qin J, Wang X, Jiang Z, Benedix F, Franke S, Wartman T, *et al*: miR-221 mediates chemoresistance of esophageal adenocarcinoma by direct targeting of DKK2 expression. *Ann Surg* 264: 804-814, 2016.



This work is licensed under a Creative Commons Attribution-NonCommercial-NoDerivatives 4.0 International (CC BY-NC-ND 4.0) License.

RETRACTED